Active Locomotive Intestinal Capsule Endoscope (ALICE) System: A Prospective Feasibility Study

Cheong Lee, Hyunchul Choi, Gwangjun Go, Semi Jeong, Seong Young Ko, Jong-Oh Park, and Sukho Park, *Member, IEEE*

***Abstract*—Owing to the limitations of the conventional flexible endoscopes used in gastrointestinal diagnostic procedures, which cause discomfort and pain in patients, a wireless capsule endoscope has been developed and commercialized. Despite the many advantages of the wireless capsule endoscope, its restricted mobility has limited its use to diagnosis of the esophagus and small intestine only. Therefore, to extend the diagnostic range of the wireless capsule endoscope into the stomach and colon, additional mobility, such as 3-D locomotion, and steering of the capsule endoscope, is necessary. Previously, several researchers reported on the development of mobility mechanisms for the capsule endoscope, but they were unable to achieve adequate degrees of freedom or sufficiently diverse capsule motions. Therefore, we proposed a novel electromagnetic actuation system that can realize 3-D locomotion and steering within the digestive organs. The proposed active locomotion intestinal capsule endoscope (ALICE) consists of five pairs of solenoid components and a capsule endoscope with a permanent magnet. With the magnetic field generated by the solenoid components, the capsule endoscope can perform various movements necessary to the diagnosis of the gastrointestinal tract, such as propulsion in any direction, steering, and helical motion. From the results of a basic locomotion test, ALICE showed a propulsion angle error of less than 4° and a propulsion force of 70 mN. To further validate the feasibility of ALICE as a diagnostic tool, we executed *ex vivo* testing using small intestine extracted from a cow. Through the basic mobility test and the *ex vivo* test, we verified ALICE's usefulness as a medical capsule endoscopic system.**

***Index Terms*—Capsule endoscope, electromagnetic, helical motion, locomotion, propulsion, steering.**

I. Introduction

In recent years, owing to irregular dietary habits, insufficient exercise, and the stress of modern society, the incidence of gastrointestinal diseases has increased. Flexible gastrointestinal endoscopes have been widely used in the prophylaxis and diagnosis of diseases of the digestive organs. However, because the flexible endoscope is inserted into either the mouth or the anus, the endoscopic procedure can be very difficult for the physician, and can cause severe pain and discomfort to the patient. In addition, the anesthetic drugs administered with the endoscopic procedures may generate serious side effects in patients [1], [2].

In an attempt to remedy the limitations of the flexible endoscopy, a capsule endoscope was proposed and developed; several companies, such as Given Imaging [3] and Intromedic [4], have commercialized this type of endoscope. PillCam SB, PillCam ESO, and PillCam COLON of Given Imaging and MiroCam SB of Intromedic have been widely used for the diagnosis in gastrointestinal tracts. The commercial capsule endoscope is the size of a pill and can be swallowed through the mouth. It moves along the esophagus, stomach, small intestine, and colon, and as it does, it takes continuous images of the inside wall of the digestive tract. The captured images are then transmitted to data storage, via an external data receiving device outside of the human body. The capsule endoscope is then extracted, and the stacked images are analyzed and diagnosed by physicians.

Because the conventional capsule endoscope does not have its own actuator it can only move passively, via the peristaltic movement of the digestive organs. Therefore, it is impossible for a physician involved in the diagnostic procedure to perform active checkups using the capsule endoscope. In addition, a great deal of time is required to review the enormous amount of stacked image data from the capsule endoscope. Moreover, because the stomach and colon have a large volume and many folding structures, it is hard to come to a precise diagnosis related to the stomach and colon using the conventional capsule endoscope. Ideally, the capsule endoscope should have its own locomotion and a steering function so that the physician can actively control it and effectively diagnose diseases of the digestive organs [1], [2], [5].

The studies on locomotive capsule endoscopes can be categorized as crawling mechanical actuation, magnetic oscillatory propulsion, or magnetic manipulation. Initially, Valdastri *et al.* [6], Kim *et al.* [7], and Kim *et al.* [8] proposed crawling mechanisms, using micromotors, gears, and screws for the capsule endoscope. However, because it was hard to miniaturize and had power limitations, the crawling mechanisms could not be applied to a real capsule endoscope.

Next, Morital *et al.* [9] and Kósa *et al.* [10] proposed self-propelled capsule endoscopes with a fin using magnetic oscillatory propulsion. They generated the oscillatory motions of the fin from the external magnetic field and propelled the capsule endoscope by propulsion from the oscillatory fin. However,

Manuscript received February 6, 2014; revised August 26, 2014; accepted October 1, 2014. Date of publication November 14, 2014; date of current version August 24, 2015. Recommended by Technical Editor F. Carpi. This work was supported by the Industrial Strategic Technology Development Program (Grant 10030037, CTO Therapeutic System) funded by the Ministry of Trade, Industry and Energy (MOTIE, Korea).

C. Lee, H. Choi, G. Go, and S. Y. Ko are with the School of Mechanical Engineering, Chonnam National University, Gwangju 500-757, Korea (e-mail: vdkqydh@naver.com; anubis_jjang@hanmail.net; gwangjun124@gmail.com; sko@jnu.ac.kr).

S. Jeong is with the Robot Research Initiative, Chonnam National University, Gwangju 500-757, Korea (e-mail: semi@jnu.ac.kr).

J.-O. Park and S. Park are with the School of Mechanical Systems Engineering, Chonnam National University, Gwangju 500-757, Korea (e-mail: jop@jnu.ac.kr; spark@jnu.ac.kr).

This paper has supplementary downloadable material available at http://ieeexplore.ieee.org provided by the authors. This includes several elementary experiments and ex-vivo tests, which can show the mobility of ALICE. This material is 29.3 MB in size. Contact spark@jnu.ac.kr for further questions about this work.

Color versions of one or more of the figures in this paper are available online at http://ieeexplore.ieee.org.

Digital Object Identifier 10.1109/TMECH.2014.2362117

these capsule endoscopes are only able to move in a fluid environment, and it was thought that the oscillatory motion might have a negative effect on the quality of the captured images.

Finally, there have been many studies on the magnetic manipulation of wireless microrobots. Martel *et al.* [11] and Ishiyama *et al.* [12] proposed spiral-type microrobots, and demonstrated their 3-D forward/backward motion through the directional control of a rotational magnetic field, using uniform magnetic field coils. The microrobots are able to obtain their propulsion force from the interaction between the threads of the spiral-type microrobots, and the inner surface of the narrow gastrointestinal tract. However, it is difficult when the spiral-type microrobot moves on a slippery surface, such as the gastric organs, or in an environment where there is no surrounding medium.

Ciuti *et al.* [13] and Carpi *et al.* [14], [15] proposed a method for controlling a capsule endoscope with a small permanent magnet, using either a robotic arm or the conventional Stereotaxis equipment. In the proposed system, large permanent external magnets are attached to the robotic arm or to the Stereotaxis equipment. The conventional Stereotaxis system also consists of two robotic arms which can manipulate the large permanent magnets, and an X-ray fluoroscope. They are therefore able to control the capsule endoscope with a small permanent magnet through the rotation and the positioning of the external large permanent magnets, using the robotic arms. Because two permanent magnets are used for the generation of the magnetic field in the region of interest (ROI), the capsule endoscope will have a smaller power consumption than the electromagnetic actuation (EMA) system using coils. Similarly, Abbott *et al.* has demonstrated the manipulation of the magnetic microrobot using the permanent magnet with a robotic arm and vision system [16], [17]. The magnetic microrobot could be positioned at a certain point in 2-D or 3-D space through the vision-based control. However, because the capsule endoscope is controlled by the position and rotation of the external magnets, using the robotic arms, we can expect that the response time of the capsule motion will be slow, and that complex motions, such as helical movements, will be too difficult.

Kummer *et al.* achieved 5-DOF motions with a microrobot using their EMA system (OctoMag) with eight coils, which has an appropriate coil structure for intraocular surgery [18]. Sitti *et al.* demonstrated the stick–slip locomotion of a microrobot using the EMA system [19], [20]. When the microrobot was placed on a uniform bottom surface, the stick–slip motion of the microrobot can be generated and it can be applied to the manipulation of microparticles on a substrate. As a typical application of the micromanipulation using electromagnetic microrobot, they demonstrated the microgripper robot using soft magnet, which can manipulate the microstructures in 3-D space [21]. However, neither the OctoMag nor the EMA with the stick–slip motion of the microrobot is suited to the investigation of a long gastrointestinal tract.

Rey *et al.* [22] and Keller *et al.* [23] proposed a magnetic-guided capsule endoscope (MGCE), using an EMA system with six stationary pairs of coils. They demonstrated 5-DOF motions of the capsule endoscope in a water filled stomach. They have already carried out clinical trials in 52 cases, and we expect that MGCE is close to being commercialized.

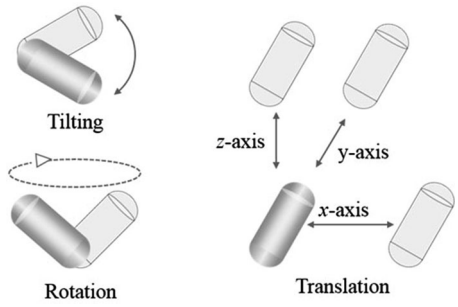

Fig. 1. Five-basic motion of the active capsule endoscope.

In this paper, we propose an active locomotion intestinal capsule endoscope (ALICE) system with diverse mobility, which is appropriate for gastrointestinal diagnosis. ALICE consists of an EMA system and capsule endoscope. The EMA system has three pairs of orthogonal uniform magnetic coils for 3-D alignment, and two pairs of gradient magnetic coils for propulsion. The MGCE consists of 12ea coils, and the coils for the alignment and the coils for the propulsion of the capsule are coupled. It is therefore very difficult to realize complex motions of the capsule, such as a helical motion. The proposed EMA system for ALICE has 10ea coils and the coils for the alignment and the coils for the propulsion of the capsule are separated. Therefore, it is very easy to realize complex motions for diagnosis when using this capsule. The ALICE capsule endoscope has a tubular shape, resulting in easy access to the patient, and achieves a 5-DOF basic motion. In addition, through the helical motion of the capsule endoscope, it is possible to closely scan the inner wall of the gastrointestinal tract and thereby to improve diagnostic efficiency. This paper consists of the following sections: Section II explains the fundamental motions of ALICE, and the structure of the EMA system. In Section III, we deal with the actuation mechanisms of the ALICE system. Section IV describes experimental setups and the results of the locomotive capsule endoscope using the ALICE system. Finally, we draw a conclusion in Section V.

II. Design of the ALICE System

A. Motion of Capsule Endoscopy

When the capsule endoscope has a cylindrical shape, and the magnetization direction is the same as the longitudinal axis of the capsule, we can derive the following actuation mechanisms: 1) rotational (tilting) motion; 2) 3-D translation motion; and 3) combined helical motion. As shown in Fig. 1, for the diagnostic purposes of a capsule endoscope, the ALICE system should realize the five basic motions, including rotational and tilting motions, and 3-D translations. In addition, through a combination of these basic motions, we propose a helical motion for the capsule endoscope. As shown in Fig. 2, the helical motion means that the capsule endoscope can be rotated and propelled simultaneously. It is anticipated that the helical motion of the capsule endoscope will be appropriate for scanning the inner walls of tubular digestive organs, such as the esophagus, small intestine, and colon.

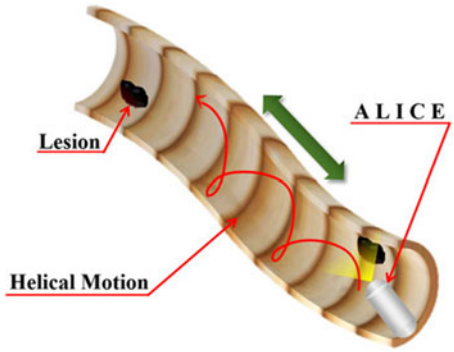

Fig. 2. Scheme of helical motion in a tubular environment.

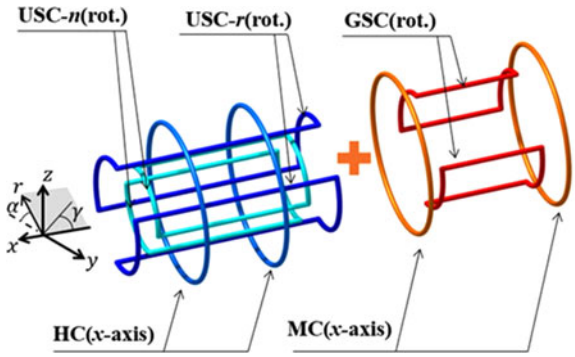

Fig. 3. Schematic diagram of the proposed EMA system.

TABLE I
CHARACTERISTIC DIMENSIONS OF THE COIL COMPONENTS OF THE ALICE SYSTEM

Coils	Radius (mm)	Turns	Resistance (Ω)
HC	195	556	13.33
MC	195	556	13.33
USC-*n*	105	334	15.56
USC-*r*	141	448	30.68
GSC	141	448	17.38

B. Design and Fabrication of the EMA System

To manage the manipulation of a capsule endoscope, the EMA system must be able to access a recumbent patient easily. Therefore, as shown in Fig. 3, the proposed ALICE system has a tubular shape, with three pairs of orthogonal uniform magnetic coil assemblies for 3-D alignment, and two pairs of gradient magnetic coil assemblies for propulsion. The ALICE system can align the capsule endoscope to a desired 3-D coordinate via Helmholtz coils (HCs) on the *x*-axis, and two rotating pairs of uniform saddle coils (USCs) on the *x*-axis, which are orthogonally positioned. In addition, the Maxwell coil (MC) and rotating gradient saddle coil (GSC) on the *x*-axis in the ALICE system can propel the capsule endoscope. The ALICE system was fabricated as shown in Fig. 3, and the detailed characteristic dimensions of the coil components are described in Table I.

III. ACTUATION MECHANISMS

A. Basic Theory of the EMA System

When a magnetic body is placed in a magnetic field, it can be aligned and propelled by magnetic torque and force [24]. The torque (τ) at which the magnetic body is aligned with the magnetic field is determined by the magnetic field vector ($\mathbf{H}$), as shown in (1). In addition, the force ($\mathbf{F}$) at which the magnetic body is propelled in the aligned direction is determined by the gradient of the magnetic field vector ($\nabla\mathbf{H}$), as shown in (2):

$$\tau = \mu_0 V \mathbf{M} \times \mathbf{H} \tag{1}$$

$$\mathbf{F} = \mu_0 V (\mathbf{M} \cdot \nabla)\mathbf{H} \tag{2}$$

where μ_0, V, and $\mathbf{M}$ denote the magnetic permeability of free space, the volume, and the magnetization value of a magnet body, respectively. Based on (1) and (2), the magnetic fields for the locomotion of the magnetic body are determined, and through the current control of the EMA system, the magnetic fields can be precisely controlled.

First, to align the magnetic body in an arbitrary but desired direction, we need a uniform magnetic field that can be generated by the HC and the USC. The HC on the *x*-axis can generate the following uniform magnetic field:

$$\mathbf{H_h} = \begin{bmatrix} d_h & 0 & 0 \end{bmatrix}^T \tag{3}$$

$$d_{\boldsymbol{h}} = 0.7155 \frac{i_h \times n_h}{r_h} \tag{4}$$

where i_h, n_h, and r_h denote the input current, turns, and radius of HC, respectively. Similarly, USC on the *y*-axis can also generate the following uniform magnetic field:

$$\mathbf{H_{usc}} = \begin{bmatrix} 0 & d_{\boldsymbol{usc}} & 0 \end{bmatrix}^T \tag{5}$$

$$d_{\boldsymbol{usc}} = 0.6004 \frac{i_{\mathrm{usc}} \times n_{\mathrm{usc}}}{r_{\mathrm{usc}}} \tag{6}$$

where i_{usc}, n_{usc}, and r_{usc} denote the input current, turns, and radius of USC, respectively. Due to the combination of these two types of uniform coils, the EMA system has a cylindrical shape and can steer the magnetic body in an arbitrary direction, with the torque calculated as in (1).

Second, the gradient magnetic fields ($\mathbf{H_m}$, $\mathbf{H_{gsc}}$) used for the propulsion of the magnetic body can be generated by the MC and the GSC, as follows:

$$\mathbf{H_m} = \begin{bmatrix} g_{\boldsymbol{m}} x & -0.5 g_{\boldsymbol{m}} y & -0.5 g_{\boldsymbol{m}} z \end{bmatrix}^T \tag{7}$$

$$g_{\boldsymbol{m}} = 0.6413 \frac{i_m \times n_m}{r_m^2} \tag{8}$$

$$\mathbf{H_{gsc}} = \begin{bmatrix} g_{\boldsymbol{gsc}} x & -2.4398\, g_{\boldsymbol{gsc}} y & 1.4398\, g_{\boldsymbol{gsc}} z \end{bmatrix}^T \tag{9}$$

$$g_{\boldsymbol{gsc}} = 0.3286 \frac{i_{\mathrm{gsc}} \times n_{\mathrm{gsc}}}{r_{\mathrm{gsc}}^2} \tag{10}$$

where i_m, n_m, and r_m are the input current, turns, and the radius of the MC and i_{gsc}, n_{gsc}, and r_{gsc} are the input current, turns, and radius of the GSC, respectively [25], [26]. Through the combination of these two types of uniform gradient coils,

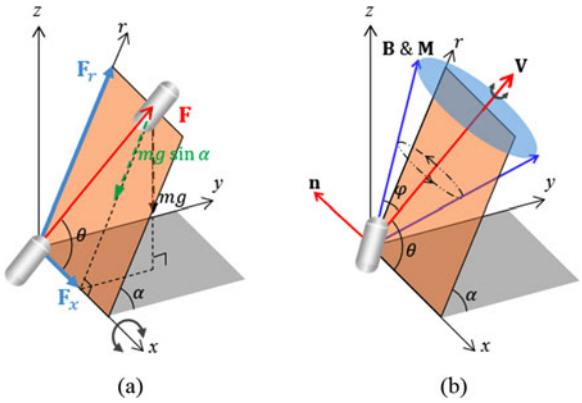

Fig. 4. Schemes of capsule endoscopic motion in 3-D space.

the EMA system can propel the magnetic body with the force given by (2) in the ROI.

B. Translation and Rotation Mechanism

First, for the translation of the capsule endoscope, we assumed that the capsule endoscope is aligned and propelled in the direction of an arbitrary angle (θ) on the *xr* plane, which is a tilted plane with a tilted angle (α) from the *y*-axis, as shown in Fig. 4(a). The virtual *xr* plane could be realized by the rotation of the saddle coils assembly. On this *xr* plane, in order to align the capsule endoscope with an arbitrary direction (θ), the magnetic fields (d_h, $d_{\mathrm{usc},r}$) from the HC and USC were determined as follows:

$$\mathbf{H} = \begin{bmatrix} d_h \\ d_{\mathrm{usc},r} \end{bmatrix} = \begin{bmatrix} B\cos\theta \\ B\sin\theta \end{bmatrix}. \tag{11}$$

In addition, the propulsion force of the capsule endoscope is derived as follows:

$$\mathbf{F} = \mathbf{F}_r + mg\sin\alpha + \mathbf{F}_x\tan\theta \tag{12}$$

where $\mathbf{F}_x$ and $\mathbf{F}_r$ denote the *x*- and *r*-directional forces that can be generated by MC and GSC, and *m* and *g* represent the mass of the capsule endoscope and the acceleration of gravity, respectively. When the relations of (7) and (9) are applied to (12), the relationship between $\mathbf{F}_x$ and $\mathbf{F}_r$ and g_{gsc} can be derived as follows:

$$\tan\theta = \frac{MV\,\sin\theta\,(-0.5\,g_m - 2.4398\,g_{\mathrm{gsc}}) - mg\sin\alpha}{MV\,\cos\theta(g_m + g_{\mathrm{gsc}})} \tag{13}$$

$$g_{\mathrm{gsc}} = -\frac{mg\sin\alpha}{3.4398} - 0.4361\,g_m. \tag{14}$$

Second, Fig. 4(b) illustrates the rotational motion of the capsule endoscope. When the capsule endoscope rotates on the vector $\mathbf{V}$ and the gradient magnetic field is applied to $\mathbf{V}$, revolution motion can be generated. The vector $\mathbf{V}$ denotes the virtual revolution axis with θ on the *x*-axis on the *xy* plane, and β on the *xy* plane, and it has same unit vector as $\mathbf{F}$. Therefore, the revolution motion on $\mathbf{V}$ is generated through the following uniform magnetic field:

$$\mathbf{H} = \begin{bmatrix} H_x \\ H_r \\ H_n \end{bmatrix} = \begin{bmatrix} \dfrac{\cos(\varphi+\theta)+\cos(\varphi-\theta)}{2} + \dfrac{\cos(\varphi+\theta)-\cos(\varphi-\theta)}{2}\cos\omega t \\ \dfrac{\sin(\varphi+\theta)-\sin(\varphi-\theta)}{2} + \dfrac{\sin(\varphi+\theta)+\sin(\varphi-\theta)}{2}\cos\omega t \\ \sin\varphi\sin\omega t \end{bmatrix} \tag{15}$$

where φ and ω are the tilting angle and the rotational period, respectively.

C. Helical Motion

To create the helical motion of the capsule endoscope, its rotational motion should follow the direction of the central axis. For its motion in the direction of an arbitrary vector ($\mathbf{V}$), the gradient magnetic field in the vector $\mathbf{V}$ should be generated through MC and GSC, and their applied currents have the relationship shown in (14). In addition, the dependent gradient magnetic field is generated in the perpendicular direction with the vector $\mathbf{V}$, and it creates a radial force that can move out of the perpendicular direction of the moving direction, following the helical track. When these two motions are combined, the capsule endoscope can move in an arbitrary direction with a helical motion, as shown in Fig. 4(b).

IV. Experiments

A. Experimental Setup

In order to evaluate the proposed ALICE system, an experimental setup was constructed, as shown in Fig. 5. The experimental setup consisted of EMA coils, a capsule endoscope model, power suppliers and a rotational motor, a controller, and a position recording part with a camera. The power suppliers were an MX12 (3EA) and 3001LX (2EA) from California Instruments, and the rotational motor was a motor-encoder-gear assembly (model number: 356846) from Maxon. The power suppliers and the rotational motor were controlled by LabVIEW 2012 and the Universal Motion Interface from National Instruments. For the motion control of the capsule endoscope, we used a conventional joystick controller (Logitec, Extream 3D Pro) and a position recording camera (Canon, 600D). The capsule endoscope model included a permanent magnet with a cylindrical shape, made of neodymium (M = 955 000 A/m); it was 6 mm in diameter and 12 mm in length. In addition, the magnetization direction was the same as that of the axis of the capsule endoscope model. Finally, a capsule endoscope model of 8 mm in diameter and 20 mm in length was fabricated by a rapid prototype method, and the permanent magnet was assembled in the capsule endoscope model.

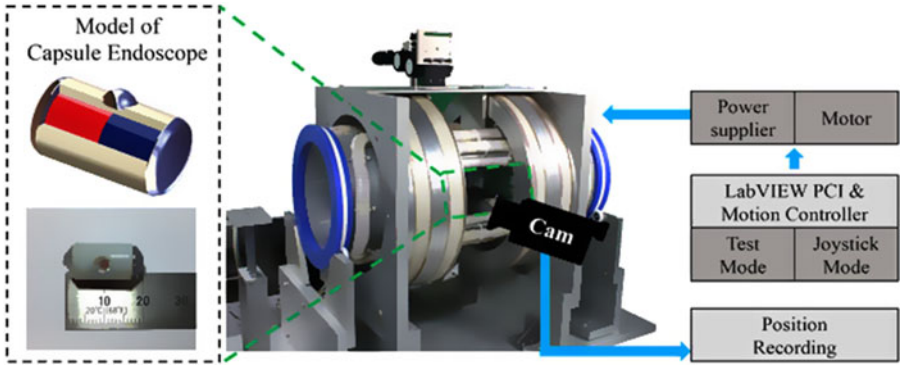

Fig. 5. Experimental setup with the ALICE system, capsule endoscope, and control process.

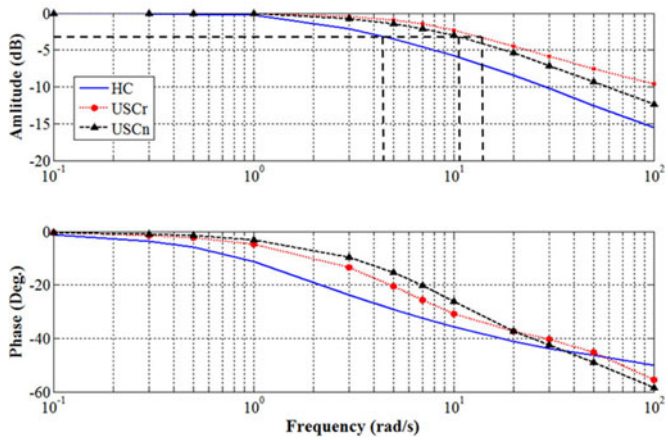

Fig. 6. Frequency response of the proposed EMA system.

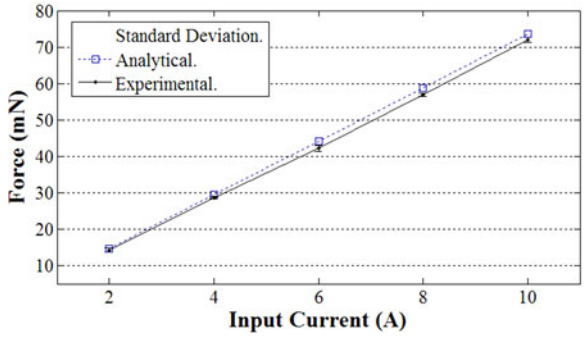

Fig. 7. Propulsion force analysis of capsule endoscope.

B. Basic Test of the EMA System

For the rotational motion of the capsule endoscope, the ALICE system used three pairs of uniform coils (one HC and two USCs). Through the bode plot of the uniform coils, we could estimate the rotational motion of the capsule endoscope as the rotating frequency increased. Fig. 6 shows the magnitude and phase plots of the three uniform coils, which were measured by an *RLC* meter (HOIKI 3522-50). Compared with the two USCs, the HC has a worse frequency response, but together the three coils can generate sufficient magnitude and phase of the rotating magnetic field until 4 Hz is achieved. We therefore expected that the capsule endoscope could be rotated by the ALICE system in the frequency range.

To further characterize the ALICE system, we measured the propulsion force of the capsule endoscope using a thread and a load cell sensor. The load cell (GSO-100, Transducer Techniques) had a range of 10 gf. However, because the generated magnetic field in the EMA coils can have considerable side effects on the load cell, the capsule endoscope was connected to the load cell using the thread. The capsule endoscope hung from the load cell through the thread, and was placed at the center of the generated magnetic field, and a glass tube of 20 mm in diameter was used to hold the capsule endoscope to the z-axis. When we changed the input current of the GSC from 0 to 10 A, with the interval of 2 A, the propulsion forces of the ALICE system were measured and compared with the analytic values. Fig. 7 shows the measured propulsion force and analytic force of the ALICE system. As the input current increased, the propulsion force also increased steadily and the maximum propulsion force was about 71.9 mN at 10 A (maximum input current). However, there were some differences between the measurement values and the analytic propulsion forces. It is expected that the difference originated from the magnetization value error of the permanent magnet in the capsule endoscope and the modeling uncertainty of the ALICE coils.

C. 5-DOF Test

First, we executed a 5-DOF Test of the capsule endoscope using the ALICE system. The capsule endoscope placed in a cubic chamber filled with silicone oil (50cS) showed translational motions of the x-, y-, and z-axes, and rotational (tilting) motions of the z- and y-axes, which are necessary motions for diagnosis when using a capsule endoscope. Fig. 8 shows the top and side views of the 5-DOF basic motions. To evaluate the steering and propulsion performance of the ALICE system, we tested the locomotion of the capsule endoscope on a 2-D plane. The test bed was an acrylate plate of 85×75 mm^2, covered by silicone oil of 2 mm thickness, which reduced the friction between the capsule endoscope and the bottom surface. We found that the capsule endoscope could be aligned to the desired direction on the 2-D plane using HC and one USC (USC-r); it could also

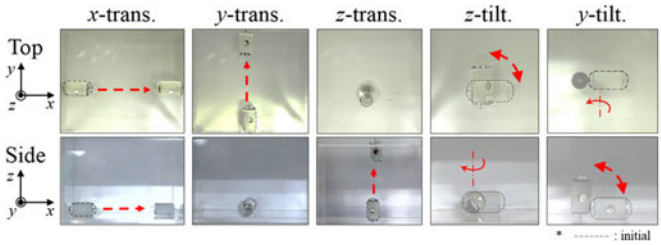

Fig. 8. Five-basic motions of capsule endoscope.

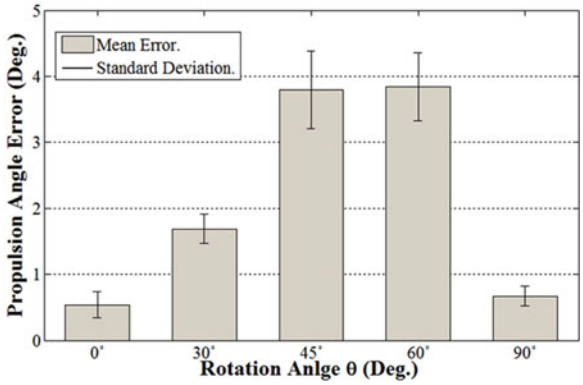

Fig. 9. Propulsion angle evaluation of capsule endoscope on a planar surface.

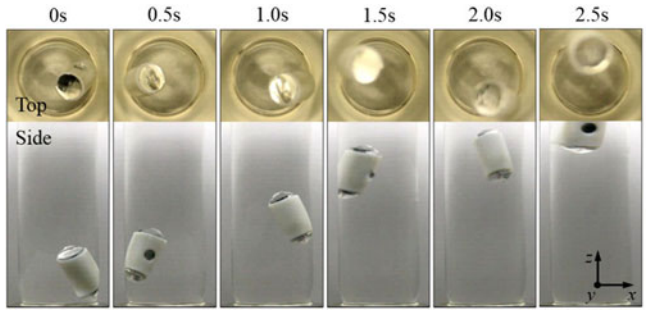

Fig. 10. Helical motion of capsule endoscope in a tubular environment.

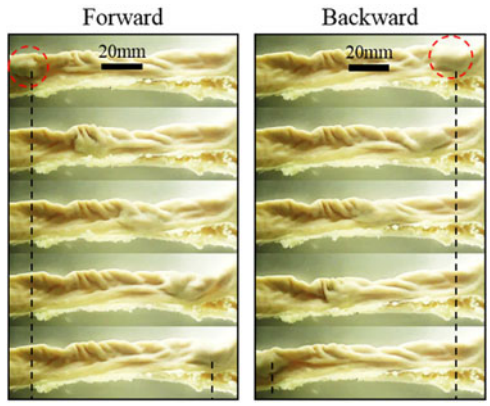

Fig. 11. Translation of capsule endoscope in a collapsed small intestine in a water bath with 90 mm depth.

be propelled in the aligned direction using MC and GSC in all angle ranges. In addition, we executed propulsion angle tests on the ALICE system using the alignment angles of 0°, 30°, 45°, 60°, and 90°.

Fig. 9 shows the propulsion angle error of the capsule endoscope in the ALICE system. The average propulsion angle error was about 3.84° and the maximum error was about 4.41°, at an alignment angle of 60°. For a capsule endoscope, propulsion angle errors of less than 4° are negligible in winding digestive organs.

D. Basic Helical Motion on z-Axis

The helical motion of the capsule endoscope on the z-axis was realized by combining the 1-D translation and the rotational motion. As a tubular phantom in this experiment, we adopted a glass tube with an inner diameter of 15 mm, filled with silicone oil of 50cS. Fig. 10 shows the helical motion of the capsule endoscope on the z-axis. A precessional uniform magnetic field on the z-axis with a tilting angle of 20° was generated through the HC and two USCs (USC-n and USC-r), thereby creating the rotation of the capsule endoscope around the z-axis. When the ascending motion of the capsule endoscope on the z-axis, using the GSCs, was combined with its rotational motion, the helical motion of the capsule endoscope could be realized. In particular, because of the centrifugal force of the rotational capsule endoscope around the z-axis, the capsule endoscope was pressed against the inner wall of the tubular phantom. This indicates that the helical motion of the capsule endoscope could be useful for accurate diagnosis of the tubular digestive organs, such as the esophagus, small intestine, and colon.

E. Ex vivo Test

First, we tested the propulsion of the capsule in an extracted and collapsed intestinal organ through the magnetic actuating force, using the ALICE system. In order to set up the intra-abdominal pressure condition, the intestine was submerged in a water bath with 90 mm depth, where the depth of water bath was calculated with the intra-abdominal pressure of the reference [27]. Fig. 11 shows sequential pictures of the forward and the backward motions of the capsule endoscope. The collapsed small intestine had a 30–40 mm width, and the total moving distance was about 80 mm. It showed an average moving velocity of 3 mm/s. Because the intestinal tract has a very slippery surface, the propulsion force of the capsule using the ALICE system must be sufficiently large for locomotion in the *ex vivo* test using the extracted intestinal tract. For a feasibility test of a practical procedure using the ALICE system, we tested the mobility of the capsule endoscope in a real digestive organ. We used a small intestine sample extracted from a cow; the sample length was about 17 cm. The intestine sample was inflated to create a similar situation to a real procedure, and a Camscope (Sometech Vision) was connected to the end of the sample to monitor the motions of the capsule endoscope. Fig. 12 show time-lapse

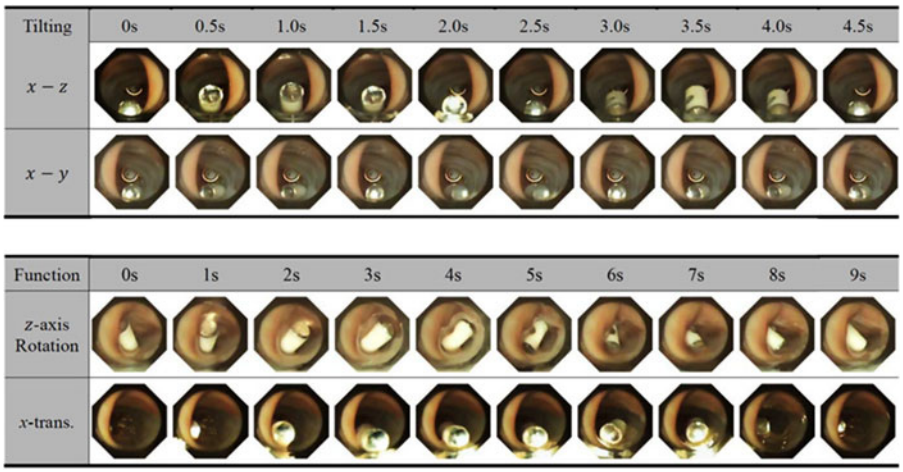

Fig. 12. Tilting, rotation, and translation motion of capsule endoscope in an inflated small intestine.

images of the tilting motions of the capsule endoscope on the *xy* and *yz* planes. In addition, the capsule endoscope could revolve on the *z*-axis and move back and forth. The motions of the capsule endoscope using the ALICE system are clearly illustrated in the supplementary video. Through a combination of the basic motions of the capsule endoscope, we were able to demonstrate the feasibility of the ALICE system for exploring real digestive organs.

V. Conclusion

In this paper, we proposed the ALICE system to improve the mobility of a capsule endoscope. Compared with previous studies on locomotive mechanisms for capsule endoscopes, the ALICE system realized various types of mobility and demonstrated feasible motion for the diagnosis of digestive organs. We proposed the EMA system using the proposed coil assembly, and then executed basic locomotive tests for the evaluation of the ALICE system. In addition, we proposed the helical motion of the capsule endoscope, which is appropriate in the diagnosis of tubular digestive organs such as the esophagus, small intestine, and colon. Finally, through *in vitro* experiments, we verified the feasibility of the ALICE system as a diagnostic apparatus. Consequently, this study demonstrated the viability of a locomotive function in a biomedical capsule endoscope. In future, if additional functions were to be developed and integrated into the capsule endoscope, such as biopsy and drug delivery, it would become a very powerful theranostic tool for the digestive organs. Generally, the radius of the MRI bore is about 350–400 mm, which is 2.5 times larger than the present EMA system. For clinical application in humans, the EMA system should be enlarged by 2.5 times. Therefore, for the generation of a similar magnetic field, the uniform coils would need 2.5 times larger currents (or number of coil turns) and the gradient coils would need 5.66 times larger currents (or number of coil turns), compared with the present EMA system. For the reliable diagnosis and the precise positioning of an active locomotive capsule endoscope, its real-time localization is very important task and ongoing research.

References

[1] V. K. Sharma, "The future is wireless: Advances in wireless diagnosis and therapeutic technologies in gastroenterology," *Gastroenterology*, vol. 137, no. 2, pp. 434–465, 2009.

[2] G. Pan and L. Wang, "Swallowable wireless capsule endoscopy: Progress and technical challenge," *Gastroenterol. Res. Pract.*, vol. 2012, pp. 1–9, 2012.

[3] G. Iddan, G. Meron, A. Glukhovsky, and P. Swain, "Wireless capsule endoscopy," *Nature*, vol. 405, p. 417–418, 2000.

[4] S. Bang, J. Park, S. Jeong, Y. Kim, H. Shim, T. Kim, D. Lee, and S. Song, "First clinical trial of the 'MiRo' capsule endoscope by using a novel transmission technology: Electric-field propagation," *Gastrointestinal Endoscopy*, vol. 69, no. 2, pp. 253–259, 2009.

[5] A. Moglia, A. Menciassi, M. O. Schurr, and P. Dario, "Wireless capsule endoscopy: From diagnosis devices to multipurpose robotic systems," *Biomed. Microdevices*, vol. 9, no. 2, pp. 235–243, 2007.

[6] P. Valdastri, R. J. Webster, C. Quaglia, M. Quirini, A. Menciassi, and P. Dario, "A new mechanism for mesoscale legged locomotion in compliant tubular environments," *IEEE Trans. Robot.*, vol. 25, no. 5, pp. 1047–1057, Oct. 2009.

[7] B. Kim, S. Lee, J. H. Park, and J. O. Park, "Design and fabrication of a locomotive mechanism for capsule-type endoscopes using shape memory alloys (SMAs)," *IEEE/ASME Trans. Mechatronics*, vol. 10, no. 1, pp. 77–86, Feb. 2005.

[8] H. Kim, S. Yang, J. Kim, S. Park, J. Cho, J. Park, T. Kim, E. Yoon, S. Song, and S. Bang, "Active locomotion of a paddling-based capsule endoscope in an in vitro and *in vivo* experiment," *Gastrointestinal Endoscopy*, vol. 72, no. 2, pp. 381–387, 2010.

[9] E. Morita, N. Ohtsuka, Y. Shindo, S. Nouda, T. Kuramoto, T. Inoue, M. Murano, E. Umegaki, and K. Higuchi, "*In vivo* trial of a driving system for a self-propelling capsule endoscope using a magnetic field," *Gastrointestinal Endoscopy*, vol. 75, no. 4, pp. 836–840, 2010.

[10] G. Kósa, P. Jakab, F. Jólesz, and N. Hata, "Swimming capsule endoscope using static RF magnetic field of MRI for propulsion," in *Proc. IEEE Int. Conf. Robot. Autom.*, 2008, pp. 2922–2927.

[11] H. Zhou, G. Alici, T. D. Than, W. Li, and S. Martel, "Magnetic propulsion of a spiral-type endoscopic microrobot in a real small intestine," in *Proc. IEEE/ASME Int. Conf. Adv. Intell. Mechatronics*, 2012, pp. 63–68.

[12] K. Ishiyama, M. Sendoh, and K. I. Arai, "Magnetic micromachines for medical applications," *J. Magn. Magn. Mater.*, vol. 242–245, no. 1, pp. 41–46, 2002.

[13] G. Ciuti, R. Donlin, P. Valdastri, A. Arezzo, A. Menciassi, M. Morino, and P. Dario, "Robotic versus manual control in magnetic steering of an endoscopic capsule," *Endoscopy*, vol. 42, pp. 148–152, 2010.

[14] F. Carpi, N. Kastelein, M. Talcott, and C. Pappone, "Magnetically controllable gastrointestinal steering of video capsules," *IEEE Trans. Biomed. Eng.*, vol. 58, no. 2, pp. 231–234, Feb. 2011.

[15] F. Carpi and C. Pappone, "Magnetic maneuvering of endoscopic capsules by means of a robotic navigation system," *IEEE Trans. Biomed. Eng.*, vol. 56, no. 5, pp. 1482–1490, May 2009.

[16] W. Mahoney and J. J. Abbott, "Generating rotating magnetic field with a single permanent magnet for propulsion of untethered magnetic devices in a lumen," *IEEE Trans. Robot.*, vol. 30, no. 2, pp. 411–420, Apr. 2014.
[17] W. Mahoney and J. J. Abbott, "Managing magnetic force applied to a magnetic device by a rotating dipole field," *Appl. Phys. Lett.*, vol. 99, no. 13, pp. 134103-1–134103-3, 2011.
[18] M. P. Kummer, J. J. Abbott, B. E. Kratochvil, R. Borer, A. Sengul, B. J. Nelson, "OctoMag: An electromagnetic system for 5-DOF wireless micromanipulation," *IEEE Trans. Robot.*, vol. 26, no. 6, pp. 1006–1017, Dec. 2010.
[19] S. Floyd, E. Diller, C. Pawashe, and M. Sitti, "Control methodologies for a heterogeneous group of untethered magnetic micro-robots," *Int. J. Robot. Res.*, vol. 30, no. 13, pp. 1553–1565, 2011.
[20] C. Pawashe, S. Floyd, and M. Sitti, "Multiple magnetic microrobot control using electrostatic anchoring," *Appl. Phys. Lett.*, vol. 94, no. 16, pp. 164108-1–164108-3, 2009.
[21] E. Diller and M. Sitti, "Three-dimensional programmable assembly by untethered magnetic robotic micro-grippers," *Adv. Funct. Mater.*, vol. 24, pp. 4397–4404, 2014.
[22] J. F. Rey, H. Ogata, N. Hosoe, K. Ohtsuka, N. Ogata, K. Ikeda, H. Aihara, I. Pangtay, T. Hibi, S. Kudo, and H. Tajiri, "Feasibility of stomach exploration with a guided capsule endoscope," *Endoscopy*, vol. 42, no. 7, pp. 541–545, 2010.
[23] H. Keller, A. Juloski, H. Kawano, M. Bechtold, A. Kimura, H. Takizawa, and R. Kuth, "Method for navigation and control of a magnetically guided capsule endoscope in the human stomach," in *Proc. Int. Conf. Biomed. Robot. Biomech.*, 2012, pp. 859–865.
[24] G. Rizzoni, *Principles and Applications of Electrical Engineering*. New York, NY, USA: McGraw-Hill Higher Education, 2003.
[25] S. T. Lin and A. R Kaufmann, "Helmholtz coils for production of powerful and uniform fields and gradients," *Rev. Modern Phys.*, vol. 25, pp. 182–190, 1953.
[26] J. M. Jin, "Electromagnetics in magnetic resonance imaging," *IEEE Antennas Propag. Mag.*, vol. 40, no. 6, pp. 7–22, Dec. 1998.
[27] N. C. Sanchez, P. L. Tenofsky, J. M. Dort, L. Y. Shen, S. D. Helmer, and R. S. Smith, "What is normal intra-abdominal pressure?" *Amer. Surgeon*, vol. 67, no. 3, pp. 243–248, 2001.

Cheong Lee received the B.S. and M.S. degrees from the Department of Mechanical Engineering, Chonnam National University, Gwangju, Korea, in 2012 and 2014, respectively, where he is currently working toward the Ph.D. degree and is a Researcher in Robot Research Initiative.

His research interests include microrobots and medical robots.

Hyunchul Choi received the B.S. and M.S. degrees from the Department of Mechanical Engineering, Chonnam National University, Gwangju, Korea, in 2008 and 2010, respectively, where he is currently working toward the Ph.D. degree and is a Researcher in Robot Research Initiative.

His research interests include microactuators and microrobots.

Gwangjun Go received the B.S. degree from the Department of Mechanical Engineering, Chonnam National University, Gwangju, Korea, in 2013, where he is currently working toward the M.S. degree and is a Researcher in Robot Research Initiative.

His research interests include micro/nanorobots.

Semi Jeong received the B.S. and M.S. degrees from the Department of Mechanical Engineering, Wonkwang University, Iksan-si, Korea, in 2005 and 2007, respectively, and the Ph.D. degree from the Department of Mechanical Engineering, Chonnam National University, Gwangju, Korea, in 2013.

She is currently a Researcher in Robot Research Initiative. Her research interests include microactuators and medical robots.

Seong Young Ko received the B.S., M.S., and Ph.D. degrees from the Department of Mechanical Engineering, Korea Advanced Institute of Science and Technology (KAIST), Daejeon, Korea, in 2000, 2002, and 2008, respectively.

In 2008, he was a Postdoctoral Researcher in the Department of Electrical Engineering, KAIST, and from 2009 to 2011, he was a Research Associate in the Mechatronics-In-Medicine Laboratory, Department of Mechanical Engineering, Imperial College London, U.K. From October 2011, he is currently an Assistant Professor in the School of Mechanical Systems Engineering, Chonnam National University, Gwangju, Korea. His research interests include medical robotics, human–robot interaction, and intelligent control.

Jong-Oh Park received the B.S. and M.S. degrees from the Department of Mechanical Engineering, KAIST, Korea, in 1978 and 1981, respectively, and the Ph.D. degree in robotics from Stuttgart University, Germany, in 1987.

From 1982 to 1987, he was a Guest Researcher with Fraunhofer-Gesellschaft Institut fur Produktionstechnik und Automatisierung, Germany. He was a Principal Researcher at the Korea Institute of Science and Technology (KIST) from 1987 to 2005 and he was also the Director of Microsystem Research Center, KIST, from 1999 to 2005. In 2005, he moved to Chonnam National University, Gwangju, Korea, where he is currently a Full Professor in the Department of Mechanical System Engineering and the Director of Robot Research Initiative. His research interests include biomedical microrobots, medical robots, and service robots.

Sukho Park (M'11) received the B.S., M.S., and Ph.D. degrees in mechanical engineering from the Korea Advanced Institute of Science and Technology, Daejeon, Korea, in 1993, 1995, and 2000, respectively.

From 2000 to 2004, he was a Senior Research Engineer with LG Electronics Production Research Center, Korea. From 2004 to 2006, he was a Senior Researcher of the Microsystem Research Center, Korea Institute of Science and Technology. In 2006, he moved to Chonnam National University, Gwangju, Korea, where he is currently an Associate Professor in the Department of Mechanical System Engineering and a Section Head of Robot Research Initiative. His research interests include microactuator/robot and micromanipulation for biomedical instrumental applications.

IEEE/ASME TRANSACTIONS ON

MECHATRONICS

A JOINT PUBLICATION OF THE IEEE INDUSTRIAL ELECTRONICS SOCIETY, THE IEEE ROBOTICS AND AUTOMATION SOCIETY, AND THE ASME DYNAMIC SYSTEMS AND CONTROL DIVISION

OCTOBER 2015 VOLUME 20 NUMBER 5 IATEFW (ISSN 1083-4435)

PAPERS

(Contents Continued on Back Cover)

ASME SETTING THE STANDARD IEEE